

# CKD: Contrastive Knowledge Distillation from A Sample-wise Perspective

Wencheng Zhu, Xin Zhou, Pengfei Zhu, Yu Wang, and Qinghua Hu, *Senior Member, IEEE*

**Abstract**—In this paper, we present a simple yet effective contrastive knowledge distillation approach, which can be formulated as a sample-wise alignment problem with intra- and inter-sample constraints. Unlike traditional knowledge distillation methods that concentrate on maximizing feature similarities or preserving class-wise semantic correlations between teacher and student features, our method attempts to recover the “dark knowledge” by aligning sample-wise teacher and student logits. Specifically, our method first minimizes logit differences within the same sample by considering their numerical values, thus preserving intra-sample similarities. Next, we bridge semantic disparities by leveraging dissimilarities across different samples. Note that constraints on intra-sample similarities and inter-sample dissimilarities can be efficiently and effectively reformulated into a contrastive learning framework with newly designed positive and negative pairs. The positive pair consists of the teacher’s and student’s logits derived from an identical sample, while the negative pairs are formed by using logits from different samples. With this formulation, our method benefits from the simplicity and efficiency of contrastive learning through the optimization of InfoNCE, yielding a run-time complexity that is far less than  $\mathcal{O}(n^2)$ , where  $n$  represents the total number of training samples. Furthermore, our method can eliminate the need for hyperparameter tuning, particularly related to temperature parameters and large batch sizes. We conduct comprehensive experiments on three datasets including *CIFAR-100*, *ImageNet-1K*, and *MS COCO*. Experimental results clearly confirm the effectiveness of the proposed method on both image classification and object detection tasks. Our source codes will be publicly available at <https://github.com/wencheng-zhu/CKD>.

**Index Terms**—Knowledge distillation, contrastive learning, intra- and inter-sample constraint, sample-wise alignment

## I. INTRODUCTION

**K**NOWLEDGE distillation (KD) [14], [15], [68] compresses knowledge without significant performance degradation, making it possible to deploy resource-intensive models on lightweight devices [19], [40], [74]. Given the practical benefits, knowledge distillation has garnered much attention over the past decade, and numerous knowledge distillation approaches have been proposed and further introduced into a wide spectrum of tasks [5], [10], [75], such as image classification [16], [39], [71], object detection [61], [82], [87], and segmentation [45], [62], [81]. While considerable improvements have been achieved, existing knowledge distillation methods still struggle to determine what knowledge to learn and how to learn it [2], [53], [66]. Here, we posit that the student model can effectively replicate the output of the teacher model when each sample is appropriately aligned.

Wencheng Zhu, Xin Zhou, Pengfei Zhu, Yu Wang, and Qinghua Hu are with the School of Artificial Intelligence, Tianjin University, Tianjin, 300385, China. Email: wenchengzhu@tju.edu.cn; zhouxinzzz@tju.edu.cn; zhupengfei@tju.edu.cn; wangyu\_@tju.edu.cn; huqinghua@tju.edu.cn. *The corresponding author is Pengfei Zhu.*

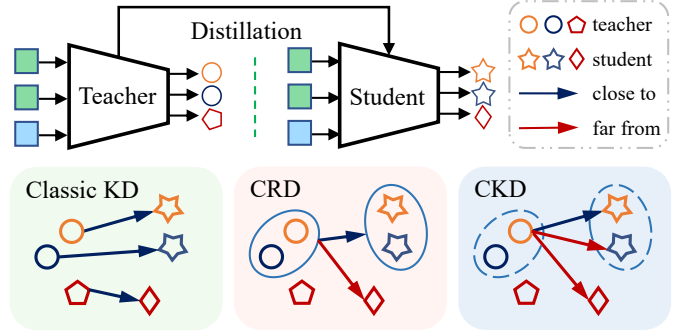


Fig. 1. Illustration of three typical approaches, including classic KD [25], CRD [70], and our CKD. Classic KD emphasizes feature similarities between teacher and student features, while CRD focuses on class-wise semantic information. In contrast, the proposed CKD conducts similarity alignment and captures sample-wise semantic structures simultaneously.

Hinton *et al.* [25] propose a seminal work on knowledge distillation, with the goal of reducing the Kullback-Leibler (KL) divergence between teacher and student logits. This influential research has led to a surge in related studies, most of which can be categorized into logit-based and feature-based approaches. Logit-based approaches distill the output logits of teachers [35], [83]. Representative methods in this category are vanilla KD [25], DML [89], DIST [26], DKD [90], etc. Following vanilla KD [25], there has been a lack of research on logit distillation, mainly because of its inferior performance relative to feature distillation. However, logits contain compact information that is easier to distill. Furthermore, logit-based methods can take advantage of low computational and storage requirements [34], [37], [86]. Our approach also employs logit distillation.

Feature-based approaches seek to replicate features extracted from intermediate layers of a teacher model [20], [42]. Typical methods include FitNet [59], OFD [24], ReviewKD [7], etc. These methods have advanced the field of knowledge distillation. However, due to rote memorization, they often suffer from severe overfitting that leads to low training losses but high test losses. Given that, RKD [55] resembles high-order structural relations among features instead of feature similarities. SP [72] preserves pairwise similarities in representation space. Although feature-based approaches effectively capture feature similarity structure, they may somewhat overlook semantic knowledge. CRD [70] innovatively distills structural representations through contrastive learning. To handle the requirement for large batch sizes in contrastive learning, CRD implements a memory buffer to enable the sampling of many negative samples, resulting in less-than-ideal training efficiency, particularly for dense

prediction tasks.

To address the aforementioned structure-preserving issues, we present a **Contrastive Knowledge Distillation** approach, dubbed CKD, which treats knowledge distillation as an intra- and inter-sample alignment problem. Fig. 1 briefly illustrates the main idea of the proposed approach in comparison with two representative approaches. We clearly observe that the proposed approach pulls logits from the same sample together while pushing logits from different samples apart. Specifically, our method assumes that a student model can well mimic a teacher model by distilling sample-wise information. This idea is straightforward and reasonable. On the one hand, previous works [7], [59] have shown tremendous success by maximizing intra-sample feature similarities. Inspired by these methods, we directly minimize logit differences within the same sample. On the other hand, solely relying on an intra-sample similarity constraint can easily lead to overfitting [57], [77]. To this end, we dive into the inter-sample constraints among different samples for additional information. Finally, we integrate these two constraints into the loss function.

Formally, the intra- and inter-sample constraints can be cast as a sample-wise contrastive learning problem. Compared to existing contrastive learning approaches [4], [70] that preserve the class-wise semantic structure, the sample-wise contrastive framework can distill teacher knowledge in an unsupervised way without label information. Moreover, our method precisely aligns teacher and student logits by exploiting both similarities and dissimilarities within each sample rather than each class. From the sample-wise perspective, this leads to a relatively small number of associated negative samples, without resorting to large batch sizes for sampling the whole negative space. Thus, the sample-wise formulation enables our approach to maintain low computational complexity in the absence of class-wise information. Furthermore, our method employs logit distillation over feature distillation for two main reasons. One reason is that logits contain high-level and compact semantic information, which is particularly suitable for contrastive learning. The other reason is that the dimension of logits, crucial for negative sampling, is lower. Notably, our method is model-agnostic and can be applied to feature distillation methods.

To sum up, the contributions of this paper are summarized into three aspects:

- 1) We present a contrastive knowledge distillation approach from the sample-wise perspective. Our method simultaneously conducts intra-sample similarity and inter-sample dissimilarity alignment between teacher and student logits.
- 2) We formulate these two intra-sample and inter-sample constraints as a contrastive learning problem with well-designed positive and negative pairs. By using the proposed contrastive formulation, our method can be efficiently and effectively trained.
- 3) We evaluate the proposed approach on benchmarks for image classification and object detection. Without bells and whistles, our approach improves the accuracy of vanilla KD by more than 1.4% and 0.98% both on the CIFAR-100 and ImageNet-1K datasets.

## II. RELATED WORK

In this section, we first outline recent progress in knowledge distillation [38], [41], [49]. Then, we review related contrastive learning approaches.

### A. Knowledge Distillation

Knowledge distillation is a representative model compression technique [49], [65], [80] that enables small models to attain strong performance of large models [1], [48], [52]. As a pioneer, Hinton *et al.* [25] introduced the concept of knowledge distillation that transfers “dark knowledge” by minimizing the KL divergence between teacher logits and student logits. Over the past few years, a rich line of knowledge distillation methods has been proposed [11], [12], [30]. These knowledge distillation methods come in two flavors: logit distillation and feature distillation [33], [50].

1) *Logit Distillation*: Earlier logit distillation approaches attempt to enhance generalization performance through regularization and optimization techniques. However, there has been limited research on early-stage logit distillation due to inferior performance. DML [89] improved the generalization abilities of networks by collaboratively training an ensemble of models through mutual learning. Instead, TAKD [51] employed multi-step distillation via intermediate-sized networks, effectively bridging the knowledge transfer gap between teacher and student networks. ICKD-C [44] utilized grid-level inter-channel correlation to capture the intrinsic distribution and diversity of feature representations. GLD [29] employed a local spatial pooling layer for the simultaneous extraction of finely localized knowledge and holistic representations. DIST [26] leveraged both inter-class and intra-class relations to align probabilistic distributions and reinforce semantic similarities, respectively. DKD [90] decoupled logits into a target class and all non-target classes, thereby enhancing both the effectiveness and flexibility of knowledge transfer. Auto-KD [35] firstly introduced an automated search strategy by employing Monte Carlo tree search to optimize knowledge distillation architectures. CTKD [39] modulated the task difficulty levels of a student network by using a dynamic and learnable temperature setting. MLKD [27] also proposed a multi-level logit distillation framework, which distills instance-level, batch-level, and class-level information. LSKD [67] considered temperature as the standard deviation of logit and applied logit standardization before the softmax prediction. Besides, there are several other studies [9], [57] devoted to explaining the basic principle of knowledge distillation. Our method belongs to logit distillation that leverages contrastive information between the logits of the teacher and student models.

2) *Feature Distillation*: Feature distillation emphasizes the maximization of similarities between intermediate representations. FitNet [59] proposed a feature-based approach that extracted trainable student representations to predict teacher representations. But, the excessive proximity between samples often results in overfitting. Hence, AT [31] mimicked attention maps of a teacher model to enhance student performance. Instead, RKD [55] transferred the relational structure among

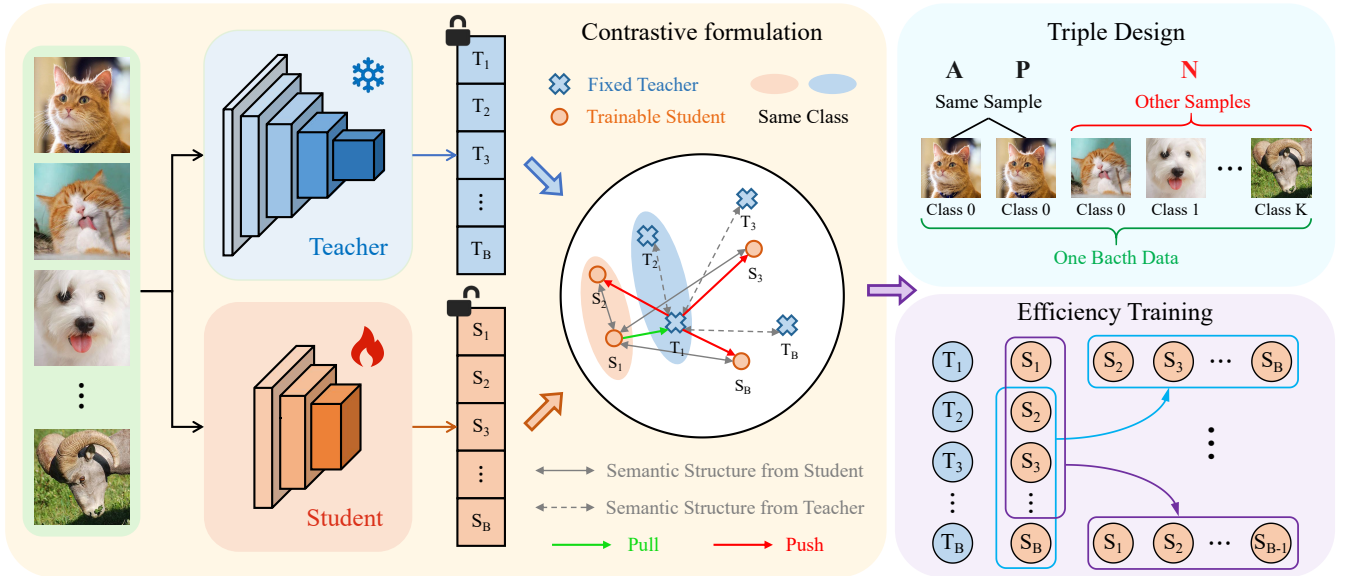


Fig. 2. The overall architecture of the proposed CKD. The newly designed triplets are introduced for similarity and semantic alignment. For example, we classify all other samples as negative, regardless of their class. In this formulation, training efficiency can be improved by reusing negative samples.

data examples by incorporating both distance-wise and angle-wise distillation objectives. IRG [46] distilled not just instance features but also the often-overlooked instance relationships and cross-layer feature transformations. CCKD [56] captured both instance-level information and correlations between multiple instances for knowledge transfer. SP [72] introduced a similarity-preserving loss to maintain the activation pattern similarities of input pairs. OFD [24] combined a new margin ReLU, an optimized distillation feature position, and a selective L2 distance to enhance network compression. CRD [70] was the first contrastive distillation approach that preserves structural representations among features. ReviewKD [7] distilled feature representations from cross-level connection paths to guide the learning of a student model. SimKD [6] reused the teacher’s classifier and introduced an additional projector to align student features. CAT-KD [17] enhances knowledge distillation’s interpretability by distilling class activation maps. This approach empowers the student model to identify discriminative regions, improving its performance. Feature-based approaches usually outperform logit-based approaches at the expense of additional computational and storage overhead.

### B. Contrastive Learning

Contrastive learning stands out as a powerful and popular branch of self-supervised learning, and plenty of efforts have been devoted to contrastive learning [3], [23]. We merely review relevant works concerned with NCE and InfoNCE.

Gutmann *et al.* [18] firstly proposed the theory of noise-contrastive estimation, in which the model learns to discriminate between samples from the actual data distribution and those from a noise distribution, thereby revealing distinct features of the data. In noise-contrastive estimation, increasing the volume of negative samples can largely reduce reliance on the quality of the noise distribution. Sohn *et al.* [64] became the first to introduce the multi-class N-pair loss for deep metric learning.

This approach eliminates the necessity to recalculate embedding representations in every iteration by allowing the reuse of embedding representations from negative samples. InstDisc [78] incorporated a memory bank mechanism that retains instance features from the preceding update step, facilitating negative sampling through integration with this non-parametric memory bank. CPC [54] popularized the InfoNCE loss for contrastive representation learning, which enhances similarities between a sample and its corresponding positive samples while decreasing similarities with negative samples. Likewise, CMC [69] leveraged a contrastive loss function to optimize the mutual information across different view representations of the same sample. MoCo [21] implemented a moving average of model parameters to update a dynamic dictionary using a queue. SimCLR [8] employed data augmentation to generate varied inputs of the same image and employed a contrastive loss to enhance the similarity between representations with different augmentations. CLIP [58] proposed a large-scale multimodal model pre-trained through the joint training of a text encoder and an image encoder with the InfoNCE loss. Previous methods have witnessed the success of contrastive learning. However, most contrastive learning approaches require substantial batch sizes of negative samples to optimize training. In this paper, we harness the potential of contrastive learning and design sample-wise triples for efficient and effective training.

## III. APPROACH

In this section, we first describe some notations. Then, we delve into contrastive knowledge distillation. Lastly, we provide a discussion about the proposed method.

### A. Notations

Knowledge distillation tasks aim to transfer knowledge from the teacher model  $\mathcal{T}$  to the student model  $\mathcal{S}$ . To be specific, given inputs  $\mathcal{X} = [\mathbf{x}_0, \mathbf{x}_1, \dots, \mathbf{x}_{n-1}]$ , we calculate teacher



logits  $\mathbf{T} = \mathcal{T}(\mathcal{X}; \theta_{\mathcal{T}})$  and student logits  $\mathbf{S} = \mathcal{S}(\mathcal{X}; \theta_{\mathcal{S}})$ , where  $\mathbf{T} = [t_0, t_1, \dots, t_{n-1}] \in \mathbb{R}^{c \times n}$  and  $\mathbf{S} = [s_0, s_1, \dots, s_{n-1}] \in \mathbb{R}^{c \times n}$ . Here,  $\theta_{\mathcal{T}}$  and  $\theta_{\mathcal{S}}$  are model parameters.  $t_i$  and  $s_i$  represent the teacher and student logits for the  $i$ -th sample in which  $i \in \mathcal{D}$ ,  $\mathcal{D} = [1, 2, \dots, n-1]$ .  $n$  denotes the sample count and  $c$  signifies the logit dimension that corresponds to the number of classes. Formally, the objective of knowledge distillation approaches can be written as:

$$\mathcal{L} = \mathcal{L}_{\text{Task}} + \alpha \mathcal{L}_{\text{KD}}. \quad (1)$$

$\mathcal{L}_{\text{Task}}$  represents the standard cross-entropy loss for image classification, and  $\alpha$  balances the classification loss  $\mathcal{L}_{\text{Task}}$  and the distillation loss  $\mathcal{L}_{\text{KD}}$ . In what follows, we elaborate on the proposed knowledge distillation loss  $\mathcal{L}_{\text{KD}}$ .

### B. Contrastive Knowledge Distillation

Generally, traditional knowledge distillation methods highlight class-level contrastive information and capture intra-class and inter-class relationships. Differently, our method focuses on sample-level representations. To be specific, the proposed approach aligns a student logit  $s_i$  with its corresponding teacher logit  $t_i$  while pushing it apart from other negative logits  $s_j$ . To achieve this goal, we endeavor to distill not only intra-sample numerical similarities but also inter-sample semantic structure. Fig. 2 presents the overall architecture of CKD. We can see that our method conducts intra-sample distillation and inter-sample distillation. Afterward, we describe these constraints in detail.

1) *Intra-Sample Distillation*: Class-wise methods usually minimize intra-class distances among samples for knowledge transfer. By adhering to these methods, the proposed approach maximizes similarities between teacher and student logits for each sample while leveraging sample-wise information. Here, we utilize the intra-sample loss, denoted as  $\mathcal{L}_{\text{intra}}$ , to optimize parameters of the student model  $\mathcal{S}$ , where  $d(\cdot, \cdot)$  represents a distance metric. Hence, we derive:

$$\begin{aligned} \mathcal{L}_{\text{intra}} &= \frac{1}{n} \sum_{i=0}^n d(t_i, s_i) \\ &= \mathbb{E}_{\mathbf{x}_i \sim \mathcal{X}} d(t_i, s_i). \end{aligned} \quad (2)$$

For  $\mathbf{x}_i \in \mathcal{X}$ , we obtain  $t_i = \mathcal{T}(\mathbf{x}_i; \theta_{\mathcal{T}})$  and  $s_i = \mathcal{S}(\mathbf{x}_i; \theta_{\mathcal{S}})$ , where  $\mathbf{x}_i \sim \mathcal{X}$  denotes a data point  $\mathbf{x}_i$  sampled from  $\mathcal{X}$ . The loss function  $\mathcal{L}_{\text{intra}}$ , defined in Eq. (2), forces the student logit  $s_i$  to approximate its analytical solution  $t_i$ . Previous studies [55], [59] have shown that continuously minimizing the gap between teacher and student representations can lead to overfitting and reduced generalization to unseen data. This is evident in the significant discrepancy between training and validation losses, especially when relying solely on intra-sample similarities.

Fig. 3 provides a detailed analysis and visualization of the intra-sample constraint on logits  $t_i$ ,  $t_j$ , and  $s_i$ . The error between the  $i$ -th teacher and student logits is represented as  $\epsilon_i = t_i - s_i$ , where  $t_i \neq t_j$ . The objective  $\mathcal{L}_{\text{intra}}$  cannot guarantee  $\forall i, d(t_i, s_i) > d(t_j, s_i)$ . Therefore, there exist errors  $\epsilon_i$ , such that  $\exists i, d(t_i, s_i) > d(t_j, s_i)$ . This inequality suggests that the student logit  $s_i$  may be closer to a teacher logit  $t_j$  than its corresponding teacher logit  $t_i$ .

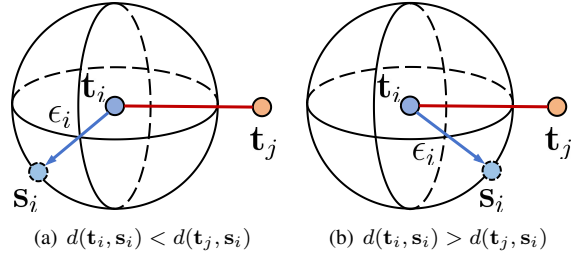


Fig. 3. Visualization of the intra-sample alignment. For the sake of simplicity, we assume that the dimension of logits is 3. The spherical surface represents  $s_i$  satisfying the condition  $\epsilon_i = t_i - s_i$  for the fixed  $\epsilon_i$ .

Formally, we assume that there are hyperplanes  $\mathcal{H}^{(k)}$ ,  $k \in \mathbb{N}$  related to  $s_i^{(k)} \in \mathcal{H}^{(k)}$ ,  $i \in \mathcal{D}$  with the same loss value, that is:

$$\forall k, h \sum_{i \in \mathcal{D}} d(t_i, s_i^{(k)}) = \sum_{i \in \mathcal{D}} d(t_i, s_i^{(h)}). \quad (3)$$

The hyperplane  $\mathcal{H}^{(k)}$  is defined as:

$$\mathcal{H}^{(k)} : \mathbf{w}^{(k)} s_i^{(k)} + b^{(k)} = 0, \quad i \in \mathcal{D}, \quad (4)$$

where  $\mathbf{w} \in \mathbb{R}^c$  is a normal vector and  $b$  is a bias.

Consider a two-dimensional plane  $y = x$  and a teacher logit  $[0.5, 0.5]$ . Despite student logits  $[0.4, 0.4]$  and  $[0.6, 0.6]$  yielding equal losses under the mean square error metric, they convey different meanings. Specifically, the logit  $[0.4, 0.4]$  lies below the decision plane, while  $[0.6, 0.6]$  lies above it. This highlights potential overfitting in intra-sample distillation. To address this, additional constraints are necessary.

2) *Inter-Sample Distillation*: Knowledge distillation should guarantee numerical similarity and semantic consistency between teacher logits and corresponding student logits [4], [70]. However, intra-sample alignment only emphasizes numerical similarity to align target logits. We introduce another inter-sample semantic alignment to simultaneously separate the logits of different samples. The inter-sample constraint  $\mathcal{L}_{\text{inter}}$  is defined as:

$$\begin{aligned} \mathcal{L}_{\text{inter}} &= -\frac{1}{n(n-1)} \sum_{i=0}^n \sum_{j \neq i}^n [d(s_i, s_j) + d(s_i, t_j)] \\ &= -\mathbb{E}_{\mathbf{x}_i \sim \mathcal{X}, \mathbf{x}_j \sim \mathcal{X}} d(s_i, s_j) - \mathbb{E}_{\mathbf{x}_i \sim \mathcal{X}, \mathbf{x}_j \sim \mathcal{X}} d(s_i, t_j). \end{aligned} \quad (5)$$

where  $\mathbf{x}_i \neq \mathbf{x}_j$ . The objective  $\mathcal{L}_{\text{inter}}$  is to make  $s_i$  far from both  $s_j$  and  $t_j$ . As shown in Fig. 3(b), we can alleviate the misalignment of  $s_i$  and  $t_j$  with Eq. (5) by maximizing their distance simultaneously.

Generally, inter-sample pairs include  $(s_i, s_j)$  and  $(s_i, t_j)$ . We consider intra-sample pairs and can obtain triples  $(s_i, t_i, s_j)$  and  $(s_i, t_i, t_j)$ . Fig. 4 visualizes these two triple categories. Previous knowledge distillation approaches [4], [70] use both triple types for training. However, unlike these methods [8], [21], [64] in which each triple element is trainable, the teacher model remains fixed, with its output  $t_i$  unchanged. It may be questionable to simply apply these two triples in knowledge distillation methods.

To address this issue, we only use triples  $(s_i, t_i, s_j)$  during training. Fig. 4 briefly illustrates the rationale behind this

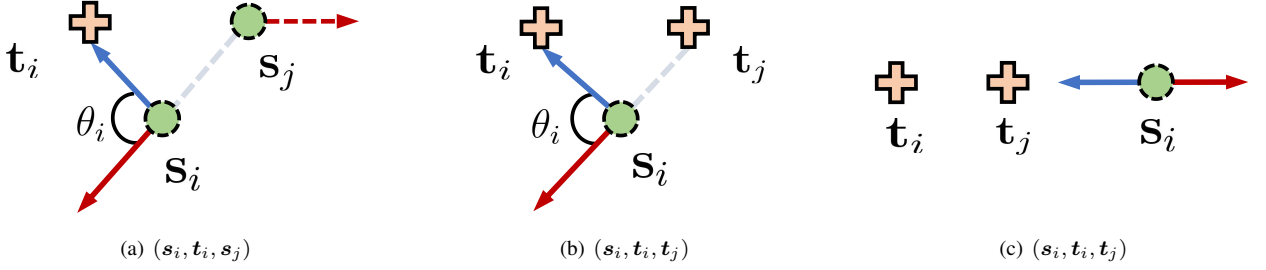


Fig. 4. Visualization of two categories of triples. (a) depicts  $(s_i, t_i, s_j)$ , while (b) and (c) show  $(s_i, t_i, t_j)$ . The blue line indicates that  $s_i$  approaches  $t_i$ , and the red line represents that  $s_i$  is far from  $s_j$  or  $t_j$ .

```

# n, b, t : number of classes, batchsize, temperature
# l_tea   : teacher logits [b, n]
# l_stu   : student logits [b, n]

# Normalization
l_tea = l2_normalize(l_tea, axis=1)
l_stu = l2_normalize(l_stu, axis=1)

# Cosine similarities
cos = np.matmul(l_tea, l_stu.T)

# Loss function : b-1 negative student samples
labels = np.arange(b)
ckd_loss = cross_entropy_loss(cos / t, labels, axis=0)

```

Fig. 5. Pseudo code of CKD in a Numpy-like style.

selection. In Fig. 4(a),  $s_i$  approaches  $t_i$  for intra-sample alignment while distancing itself from  $s_j$  for inter-sample alignment. Even with a gradient conflict when  $\theta_i > \pi/2$ , we can resolve it by adjusting  $s_j$ . However, in Fig. 4(b), the conflict remains unresolved due to the fixed  $t_j$ . Additionally, Fig. 4(c) depicts the worst-case scenario where the gradient conflict is at its maximum. From Fig. 4, we can conclude that inter-samples are crucial for model updates and the triple  $(s_i, t_i, t_j)$  may cause gradient conflicts. Thus, our method merely adopt the triple  $(s_i, t_i, s_j)$ , and the inter-sample objective is formed as:

$$\begin{aligned} \mathcal{L}_{\text{inter}} &= -\frac{1}{n(n-1)} \sum_{i=0}^n \sum_{j \neq i}^n d(s_i, s_j) \\ &= -\mathbb{E}_{x_i \sim \mathcal{X}, x_j \sim \mathcal{X}} d(s_i, s_j). \end{aligned} \quad (6)$$

Finally, we combine Eq. (2) and Eq. (6) with a tradeoff parameter  $\beta$  to obtain the following loss function:

$$\mathcal{L}_{\text{KD}} = \mathcal{L}_{\text{intra}} + \beta \mathcal{L}_{\text{inter}}. \quad (7)$$

Eq. (7) is to maximize similarities between teacher and student logits for the same sample while minimizing correlations across different samples. By pulling positive pairs closer and pushing negative pairs apart, the intra-sample and inter-sample formulations enable the alignment of teacher and student logits, ensuring they share similar semantic information for similarity and dissimilarity.

3) *Contrastive Formulation*: The proposed structure-preserving alignment shares a similar objective with contrastive learning [54], [79]. We seek to transform our objective into a sample-wise contrastive learning formulation. Specifically,  $\mathcal{L}_{\text{KD}}$  can be expressed as:

$$\mathcal{L}_{\text{KD}} = \mathbb{E}_{x_i \sim \mathcal{X}} d(t_i, s_i) - \beta \mathbb{E}_{x_i \sim \mathcal{X}} d(s_i, s_j). \quad (8)$$

For simplicity, we utilize the distance metric  $f(u, v)$  to assess the similarity between  $u$  and  $v$ , and set  $f(u, v) = -d(u, v)$ . The loss function can be derived as:

$$\mathcal{L}_{\text{KD}} = \mathbb{E}_{x_i \sim \mathcal{X}} \left[ -\left( f(t_i, s_i) - \beta \mathbb{E}_{x_j \sim \mathcal{X}} f(s_i, s_j) \right) \right] \quad (9)$$

$$= \mathbb{E}_{x_i \sim \mathcal{X}} \ln \left[ \frac{\mathbb{E}_{x_j \sim \mathcal{X}} e^{\beta f(s_i, s_j)}}{e^{f(t_i, s_i)}} + \frac{e^{f(t_i, s_i)}}{e^{f(t_i, s_i)}} - 1 \right] \quad (10)$$

$$\approx \mathbb{E}_{x_i \sim \mathcal{X}} \left[ -\ln \frac{e^{f(t_i, s_i)}}{e^{f(t_i, s_i)} + \mathbb{E}_{x_j \sim \mathcal{X}} e^{\beta f(s_i, s_j)}} \right] \quad (11)$$

$$\approx \mathbb{E}_{x_i \sim \mathcal{X}} \left[ -\ln \frac{e^{f(t_i, s_i)/\tau}}{e^{f(t_i, s_i)/\tau} + \mathbb{E}_{x_j \sim \mathcal{X}} e^{\beta f(s_i, s_j)/\tau}} \right]. \quad (12)$$

The objective can be viewed as a sample-wise contrastive loss. Here, the teacher logit  $t_i$  and its corresponding student logit  $s_i$  form a positive pair, while  $s_i$  and  $s_j$  form a negative pair. Next, we will explore the benefits of this contrastive formulation. As shown in Eq. (9), to calculate the expected value  $f(s_i, s_j)$  for each  $x_i$ , we sample negative pairs from the data space  $x_j$ . Following vanilla KD [25], we introduce a temperature parameter  $\tau$  to soften the probability distribution, satisfying Eq. (12). The parameter  $\beta$  balances the importance of positive and negative pairs, where a larger  $\beta$  is assigned when negative pairs are important; otherwise, a smaller value is preferable. Note that negative sampling can also achieve this trade-off. When the negative space is significant, we increase the sampling of negative pairs for more detailed space estimation and weight adjustment. Conversely, fewer negative samples are selected when they are less important. Contrastive learning enables efficient batch data processing in parallel. In our formulation, we construct batches of training data, each containing one positive sample and  $B - 1$  negative samples, where  $B$  is the batch size. From Fig. 2, the number of negative samples depends on  $B$ . Therefore, by varying  $B$ , we can sample

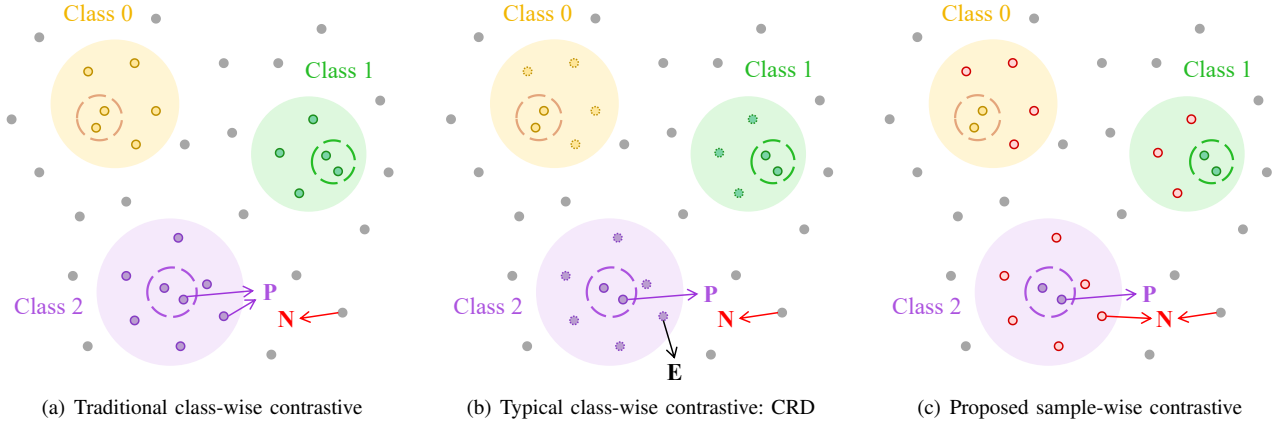


Fig. 6. Visualization of two categories of contrastive learning: Class-wise vs. Sample-wise. CRD is a typical class-wise formulation. Different background colors represent various sample categories, with P denoting positive samples and N denoting negative samples. The symbol E indicates that samples from the same class are excluded during training. The dashed circle contains teacher and student representations of the same sample

different numbers of negative samples, balancing intra-sample and inter-sample alignment.

Additionally, we substitute  $f(\mathbf{t}_i, \mathbf{s}_j)$  for  $f(\mathbf{s}_i, \mathbf{s}_j)$ . First, our method primarily aims to align  $\mathbf{s}_i$  and  $\mathbf{t}_i$ , such that  $\mathbf{t}_i = \mathbf{s}_i$ . This leads to  $\mathbf{t}_i = \mathbf{s}_i \Rightarrow f(\mathbf{t}_i, \mathbf{s}_j) = f(\mathbf{s}_i, \mathbf{s}_j)$ . Then,  $f(\mathbf{s}_i, \mathbf{s}_j)$  involves two updating variables but  $f(\mathbf{t}_i, \mathbf{s}_j)$  only has one variable, simplifying the optimization of  $\mathbf{s}_j$ . Specifically, we treat  $\mathbf{t}_i$  as an anchor logit and separately learn its positive logit  $\mathbf{s}_i$  and negative logit  $\mathbf{s}_j$ . Most importantly, this setup allows our method to leverage negative samples through the N-pair loss [64] or InfoNCE loss [54]. Similar to CLIP [58], we sample a batch of  $B$  (teacher, student) pairs with  $B \times B$  (teacher, student) pairings for efficient training.

Consequently, we derive the final loss function as,

$$\mathcal{L}_{\text{KD}} \simeq \mathbb{E}_{\mathbf{x}_i \sim \mathcal{X}} \left[ -\ln \frac{e^{f(\mathbf{t}_i, \mathbf{s}_i)/\tau}}{e^{f(\mathbf{t}_i, \mathbf{s}_i)/\tau} + \sum_{\mathbf{s}_j} e^{f(\mathbf{s}_i, \mathbf{s}_j)/\tau}} \right] \quad (13)$$

$$\simeq \mathbb{E}_{\mathbf{x}_i \sim \mathcal{X}} \left[ -\ln \frac{e^{f(\mathbf{t}_i, \mathbf{s}_i)/\tau}}{e^{f(\mathbf{t}_i, \mathbf{s}_i)/\tau} + \sum_{\mathbf{s}_j} e^{f(\mathbf{t}_i, \mathbf{s}_j)/\tau}} \right]. \quad (14)$$

In Fig. 5, we present the pseudo-code for the proposed CKD in a Numpy-like style.

**Theorem 1.** Given triples  $(\mathbf{t}_i, \mathbf{s}_i, \mathbf{s}_j)$  and the loss function  $\mathcal{L}_i$  that is defined as:

$$\mathcal{L}_i = -\ln \frac{e^{f(\mathbf{t}_i, \mathbf{s}_i)/\tau}}{e^{f(\mathbf{t}_i, \mathbf{s}_i)/\tau} + \sum_{\mathbf{s}_j} e^{f(\mathbf{t}_i, \mathbf{s}_j)/\tau}}. \quad (15)$$

The gradients  $\nabla_{\mathbf{s}_i} \mathcal{L}_i$  and  $\nabla_{\mathbf{s}_j} \mathcal{L}_i$  are proportional to  $g_i$  that is formed as:

$$g_i = 1 - \frac{e^{f(\mathbf{t}_i, \mathbf{s}_i)/\tau}}{e^{f(\mathbf{t}_i, \mathbf{s}_i)/\tau} + \sum_{\mathbf{s}_j} e^{f(\mathbf{t}_i, \mathbf{s}_j)/\tau}}. \quad (16)$$

*Proof.* The detailed proof can be found in [84].

**Theorem 2.** For class-wise contrastive learning,  $\mathbf{x}_i$  and  $\mathbf{x}_j$  belong to different classes and  $f(\mathbf{t}_i, \mathbf{s}_i) - f(\mathbf{t}_i, \mathbf{s}_j) = \rho_j$ . When we decrease  $B$ , The gradients  $\nabla_{\mathbf{s}_i} \mathcal{L}_i$  also decreases.

---

### Algorithm 1: Training procedure of the proposed CKD

---

**Input:** Images  $\mathcal{X} = \{\mathbf{x}_i\}_{i=1}^{n-1}$ , annotations  $\mathcal{Y} = \{y_i\}_{i=1}^{n-1}$ , and the teacher model  $\mathcal{T}(\mathcal{X}; \theta_{\mathcal{T}})$   
**Output:** The student model  $\mathcal{S}(\mathcal{X}; \theta_{\mathcal{S}})$   
**for**  $epoch \in \{1, 2, \dots, Epoch\}$  **do**  
  **while** Randomly sample a batch  $\mathbf{B} \in \mathcal{X}$  and  $\mathbf{y} \in \mathcal{Y}$  **do**  
    % Compute teacher and student logits  
     $\mathbf{t}_B = \mathcal{T}(\mathbf{B}; \theta_{\mathcal{T}})$   
     $\mathbf{s}_B = \mathcal{S}(\mathbf{B}; \theta_{\mathcal{S}})$   
    % Compute knowledge distillation loss  
     $\mathbf{t}'_B = \text{Normalize}(\mathbf{t}_B)$   
     $\mathbf{s}'_B = \text{Normalize}(\mathbf{s}_B)$   
     $\mathcal{L}_{\text{KD}} \leftarrow \text{SampleWiseContrastive}(\mathbf{s}'_B, \mathbf{t}'_B)$   
    % Compute classification loss  
     $\hat{\mathbf{y}} \leftarrow \text{Softmax}(\mathbf{s}_B)$   
     $\mathcal{L}_{\text{Task}} \leftarrow \text{CrossEntropy}(\hat{\mathbf{y}}, \mathbf{y})$   
    % Apply the loss in Eq. (7)  
     $\mathcal{L} \leftarrow \mathcal{L}_{\text{Task}} + \alpha \mathcal{L}_{\text{KD}}$   
     $\theta_{\mathcal{S}} \leftarrow \theta_{\mathcal{S}} - \eta \partial \mathcal{L} / \partial \theta_{\mathcal{S}}$   
  **end**  
**end**

---

*Proof.* From Eq. (16), we can obtain following equations:

$$g_i = 1 - \frac{e^{f(\mathbf{t}_i, \mathbf{s}_i)/\tau}}{e^{f(\mathbf{t}_i, \mathbf{s}_i)/\tau} + \sum_{\mathbf{s}_j} e^{f(\mathbf{t}_i, \mathbf{s}_j)/\tau}} \quad (17)$$

$$= 1 - \frac{1}{1 + \sum_{\mathbf{s}_j} e^{-\rho_j/\tau}} \quad (18)$$

$$\simeq 1 - \frac{1}{1 + B \times e^{-\rho_j/\tau}}. \quad (19)$$

When  $B$  decreases, we sample fewer negative samples, resulting in a larger  $\rho_j$  and a smaller  $g_i$ . Consequently, the gradients  $\nabla_{\mathbf{s}_i} \mathcal{L}_i$  decrease.

From Theorem 2, we can find that when positive samples and negative samples exhibit weak correlations, the value of  $f(\mathbf{t}_i, \mathbf{s}_j)$  is minimized, reducing the gradient of backpropagation  $\nabla_{\mathbf{s}_i} \mathcal{L}_i$ . This hampers model parameter updates. Therefore, class-wise methods [21], [64] heavily rely on large batch sizes to mitigate this issue and improve learning efficiency [84].

TABLE I

CLASSIFICATION ACCURACY (%) ON THE CIFAR-100 VALIDATION SET, WHERE TEACHER AND STUDENT NETWORKS SHARE THE SAME ARCHITECTURE TYPE.  $\Delta$  DENOTES THE IMPROVED PERFORMANCE COMPARED TO VANILLA KD. ALL RESULTS ARE THE AVERAGE OVER FIVE TRIALS.

Methods	Teacher	ResNet56	ResNet110	ResNet32 $\times$ 4	WRN-40-2	WRN-40-2	VGG13
	Student	ResNet20	ResNet32	ResNet8 $\times$ 4	WRN-16-2	WRN-40-1	VGG8
		72.34	74.31	79.42	75.61	75.61	74.64
		69.06	71.14	72.50	73.26	71.98	70.36
Features	FitNet [59]	69.21	71.06	73.50	73.58	72.24	71.02
	AT [31]	70.55	72.31	73.44	74.08	72.77	71.43
	RKD [55]	69.61	71.82	71.90	73.35	72.22	71.48
	CRD [70]	71.16	73.48	75.51	75.48	74.14	73.94
	OFD [24]	70.98	73.23	74.95	75.24	74.33	73.95
	ReviewKD [7]	71.89	73.89	75.63	76.12	75.09	74.84
Logits	Vanilla KD [25]	70.66	73.08	73.33	74.92	73.54	72.98
	TAKD [51]	70.83	73.37	73.81	75.12	73.78	73.23
	DKD [90]	71.97	74.11	76.32	76.24	74.81	74.68
	<b>CKD</b>	<b>72.12</b>	<b>74.48</b>	<b>76.76</b>	<b>76.28</b>	<b>75.14</b>	<b>74.98</b>
	$\Delta$	<b>+1.46</b>	<b>+1.40</b>	<b>+3.43</b>	<b>+1.36</b>	<b>+1.60</b>	<b>+2.00</b>

**Theorem 3.** For sample-wise contrastive learning,  $\exists j, \mathbf{x}_i$  and  $\mathbf{x}_j$  are in the same class, such that  $\exists j, f(\mathbf{t}_i, \mathbf{s}_i) \sim f(\mathbf{t}_i, \mathbf{s}_j)$ , large batch sizes are not crucial.

*Proof.* For sample-wise triples,  $\exists j, f(\mathbf{t}_i, \mathbf{s}_i) \sim f(\mathbf{t}_i, \mathbf{s}_j)$ , we can obtain  $\exists j, \rho_j \sim 0$  and a larger  $B \times e^{-\rho_j}$  is achieved, when we sample negative samples that are from the same class. Our method is unnecessary for comprehensive negative space sampling with large batch sizes.

Fig. 6 visualizes traditional class-wise and the proposed sample-wise formulations. Specifically, CRD [70] is a representative class-wise contrastive learning approach by using a memory bank. We can observe that class-wise formulations including CRD generate negative pairs from different classes. These negative samples often have low similarity due to varied semantic content, necessitating a larger batch size to increase  $g_i$ . In contrast, the sample-wise formulation selects negative samples from the same class, thereby exhibiting stronger relationships. Thus, our method does not require a large batch size. In fact, a large batch size can hinder our method by influencing intra-sample alignment with a large  $\beta$ . However, a small batch size may also lead to insufficient gradient magnitude.

Specifically, given the logit space  $\mathbf{T} \in \mathbb{R}^{c \times n}$ , the negative logit space for the  $i$ -th sample is denoted as  $\mathbf{T}_{/i} \in \mathbb{R}^{c \times (n-1)}$ . Assume that there are  $c$  classes, each containing  $m$  samples. We can derive:

$$\text{rank}(\mathbf{T}_{/i}) \leq \min(c, n-1) = c, \quad \text{s.t. } c \ll n. \quad (20)$$

Eq. (20) suggests that in the proposed method, the number of negative pairs sampled should heavily depend on the class number  $c$  rather than the sample number  $n$ . Taking category correlations into consideration, the actual number of negative pairs sampled should be even lower than  $c$ .

Furthermore, compared to class-wise contrastive learning approaches, our method can be efficiently trained with well-

designed triples. For classic contrastive learning methods with  $n$  samples, a total of  $\mathcal{O}(nm)$  triples should be selected for each sample:

$$\binom{m-1}{1} \binom{n-m}{1} = nm - m^2 - n + m \propto \mathcal{O}(nm) \quad (21)$$

Eq. (21) shows that for each sample, we randomly select one sample within the same class including  $m-1$  selections, and one sample from a different class, yielding a total of  $\mathcal{O}(nm)$  triples. As for CRD, we only need to select one sample from different classes because the positive pair is obtained by using the same sample:

$$\binom{1}{1} \binom{n-m}{1} = n - m \propto \mathcal{O}(n). \quad (22)$$

However, the negative space  $\mathcal{O}(n)$  is vast, necessitating the use of a memory bank with a size of  $K$ . As a result,  $K$  triples are available for training each sample. In contrast, the proposed method requires sampling only  $\mathcal{O}(c)$  triples:

$$\binom{1}{1} \binom{c}{1} = c \propto \mathcal{O}(1), \quad (23)$$

where  $c \ll n$ . We randomly shuffle data samples and select non-overlapping  $c$  samples in order. Therefore, our sample-wise formulation exhibits efficient trainability in comparison to the class-wise formulation in contrastive knowledge distillation.

To sum up, we encapsulate the training procedure in **Algorithm 1**.

## IV. EXPERIMENTS

### A. Image Classification

1) *Datasets:* We first conduct experiments on CIFAR-100 [32] and ImageNet-1K [13]. The CIFAR-100 dataset contains 100 classes, each with 600 images. The training and validation sets comprise 50K and 10K images. The ImageNet-1K dataset consists of 1000 classes. The training set has about 1.28 million images, and the validation set contains 50k images.

TABLE II

CLASSIFICATION ACCURACY (%) ON THE CIFAR-100 VALIDATION SET FOR DIFFERENT TEACHER-STUDENT NETWORK ARCHITECTURE.  $\Delta$  DENOTES THE IMPROVEMENT IN PERFORMANCE COMPARED TO VANILLA KD. RESULTS ARE AVERAGED OVER FIVE TRIALS.

Methods	Teacher	ResNet32 $\times$ 4	WRN-40-2	VGG13	ResNet50	ResNet32 $\times$ 4
	Student	ShuffleNetV1	ShuffleNetV1	MobileNetV2	MobileNetV2	ShuffleNetV2
		79.42	75.61	74.64	79.34	79.42
		70.50	70.50	64.60	64.60	71.82
Features	FitNet [59]	73.59	73.73	64.14	63.16	73.54
	AT [31]	71.73	73.32	59.40	58.58	72.73
	RKD [55]	72.28	72.21	64.52	64.43	73.21
	CRD [70]	75.11	76.05	69.73	69.11	75.65
	OFD [24]	75.98	75.85	69.48	69.04	76.82
	ReviewKD [7]	77.45	77.14	<b>70.37</b>	69.89	77.78
Logits	Vanilla KD [25]	74.07	74.83	67.37	67.35	74.45
	TAKD [51]	74.53	75.34	67.91	68.02	74.82
	DKD [90]	76.45	76.70	69.71	70.35	77.07
	<b>CKD</b>	<b>77.72</b>	<b>77.47</b>	70.11	<b>70.62</b>	<b>78.18</b>
	$\Delta$	<b>+3.65</b>	<b>+2.64</b>	<b>+2.74</b>	<b>+3.27</b>	<b>+3.73</b>

TABLE III

TOP-1 AND TOP-5 ACCURACY (%) ON THE IMAGENET-1K VALIDATION SET. RESNET-34 SERVES AS THE TEACHER, WHILE RESNET-18 ACTS AS THE STUDENT.  $\Delta$  DENOTES THE PERFORMANCE IMPROVEMENT COMPARED TO VANILLA KD. ALL RESULTS ARE THE AVERAGE OVER THREE TRIALS.

Baselines			Features				Logits			
	Teacher	Student	AT [85]	OFD [24]	CRD [70]	ReviewKD [7]	Vanilla KD [25]	DKD [90]	<b>CKD</b>	$\Delta$
Top-1	73.31	69.75	70.69	70.81	71.17	71.61	70.66	71.70	<b>72.24</b>	<b>+1.58</b>
Top-5	91.42	89.07	90.01	89.98	90.13	90.51	89.88	90.41	<b>90.81</b>	<b>+0.93</b>

TABLE IV

TOP-1 AND TOP-5 ACCURACY (%) ON THE IMAGENET-1K VALIDATION SET. RESNET-34 SERVES AS THE TEACHER, WHILE RESNET-18 ACTS AS THE STUDENT.  $\Delta$  DENOTES THE IMPROVED PERFORMANCE COMPARED TO VANILLA KD. ALL RESULTS ARE AVERAGED OVER THREE TRIALS.

Baselines			Features				Logits			
	Teacher	Student	AT [85]	OFD [24]	CRD [70]	ReviewKD [7]	Vanilla KD [25]	DKD [90]	<b>CKD</b>	$\Delta$
Top-1	76.16	68.87	69.56	71.25	71.37	72.56	68.58	72.05	<b>72.97</b>	<b>+4.39</b>
Top-5	92.86	88.76	89.33	90.34	90.41	91.00	88.98	91.05	<b>91.36</b>	<b>+2.38</b>

2) *Experimental Setup*: We evaluate eleven isomorphic or heterogeneous architectures on CIFAR-100 and compare with vanilla KD [25], AT [85], FitNet [59], RKD [55], CRD [70], OFD [24], ReviewKD [7], TAKD [51], and DKD [90].

For ImageNet-1K, we evaluate representatives, including ResNet34 & ResNet18, and ResNet50 & MobileNetV2. We provide comparisons with vanilla KD [25], AT [85], OFD [24], CRD [70], ReviewKD [7], and DKD [90]. Top-1 and top-5 recognition rates are reported.

3) *Implementation Details*: All experiments are conducted on NVIDIA RTX 3090. For CIFAR-100, we set  $\alpha$  to 100 and employ cosine annealing for learning rates. For homogeneous and heterogeneous networks, we set batch sizes to 64 and 32, with an initial learning rate of 0.05 and 0.01, respectively. For ImageNet-1K, we also use cosine annealing, with an initial learning rate of 0.2. We set  $\alpha$  to 10 and a batch size to 512.

4) *Performance on CIFAR-100*: We conduct classification experiments by using eleven combinations of isomorphic

or heterogeneous teacher and student network architectures, including ResNet [22], WideResNet [73], VGG [63], ShuffleNet [47], [88], and MobileNet [60].

Table I presents classification performance by using teacher and student architectures of the same style. We can observe that our method achieves competitive performance against feature-based and logit-based methods. Specifically, the proposed CKD improves vanilla KD accuracy by 1.36%, with a maximum gain of 3.43%. Moreover, CKD also outperforms CRD on the CIFAR-100 dataset, with an improvement of almost 1.00%.

Table II shows the classification performance of teacher-student networks with different styles. We see that our CKD method consistently yields improvements across teacher-student network pairs compared to vanilla KD. Specifically, for different architectures, CKD achieves an average improvement of 3.21% over vanilla KD, with an impressive maximum gain of 3.73%.

5) *Performance on ImageNet-1K*: To further verify the ability of CKD, we perform experiments on the ImageNet-1K



TABLE V  
OBJECT DETECTION PERFORMANCE ON THE MS-COCO DATASET. WE EMPLOY THE TWO-STAGE FASTER RCNN WITH FPN AS THE DETECTOR. TEACHER-STUDENT PAIRS ARE RESNET101 & RESNET-18, RESNET101 & RESNET50, AND RESNET50 & MOBILENETV2, RESPECTIVELY.  $\Delta$  REPRESENTS THE IMPROVED PERFORMANCE COMPARED TO REVIEWKD.

Methods	ResNet101 & ResNet18			ResNet101 & ResNet50			ResNet50 & MobileNetV2		
	AP	AP <sub>50</sub>	AP <sub>75</sub>	AP	AP <sub>50</sub>	AP <sub>75</sub>	AP	AP <sub>50</sub>	AP <sub>75</sub>
Teacher	42.04	62.48	45.88	42.04	62.48	45.88	40.22	61.02	43.81
Student	33.26	53.61	35.26	37.93	58.84	41.05	29.47	48.87	30.90
Vanilla KD [25]	33.97	54.66	36.62	38.35	59.41	41.71	30.13	50.28	31.35
FitNet [59]	34.13	54.16	36.71	38.76	59.62	41.80	30.20	49.80	31.69
FGFI [76]	35.44	55.51	38.17	39.44	60.27	43.04	31.16	50.68	32.92
ReviewKD [7]	36.75	56.72	34.00	40.36	60.97	44.08	33.71	53.15	36.13
DKD [90]	35.05	56.60	37.54	39.25	60.90	42.73	32.34	53.77	34.01
DKD+ReviewKD	37.01	57.53	39.85	40.65	61.51	44.44	34.35	54.89	36.61
<b>CKD</b>	35.08	55.47	38.01	39.71	60.64	43.31	31.72	50.01	33.62
<b>CKD+ReviewKD</b>	<b>37.65</b>	<b>57.91</b>	<b>40.71</b>	<b>41.45</b>	<b>61.93</b>	<b>45.31</b>	<b>35.31</b>	<b>55.35</b>	<b>37.88</b>
$\Delta$	<b>+0.90</b>	<b>+1.19</b>	<b>+6.71</b>	<b>+1.09</b>	<b>+0.96</b>	<b>+1.23</b>	<b>+1.60</b>	<b>+2.20</b>	<b>+1.75</b>

TABLE VI  
ABLATION STUDIES OF CONTRASTIVE FORMULATION ON THE CIFAR-100 DATASET. EXPERIMENTS ARE CONDUCTED ON HOMOGENEOUS AND HETEROGENEOUS TEACHER-STUDENT PAIRS. SUPCON AND CRD ARE CLASS-WISE METHODS, WHILE OUR CKD IS A SAMPLE-WISE APPROACH.

Methods	Homogeneous architectures			Heterogeneous architectures		
Teacher	ResNet56 72.34	WRN-40-2 75.61	WRN-40-2 75.61	VGG13 74.64	ResNet50 79.34	ResNet32 $\times$ 4 79.42
Student	ResNet20 69.06	WRN-16-2 73.26	WRN-40-1 71.98	MobileNetV2 64.60	MobileNetV2 64.60	ShuffleNetV2 71.82
SupCon [28]	69.93	75.45	74.10	67.39	67.72	75.20
CRD [70]	71.16	75.48	74.14	69.73	69.11	75.65
<b>CKD</b>	<b>72.12</b>	<b>76.28</b>	<b>75.14</b>	<b>70.11</b>	<b>70.62</b>	<b>78.18</b>

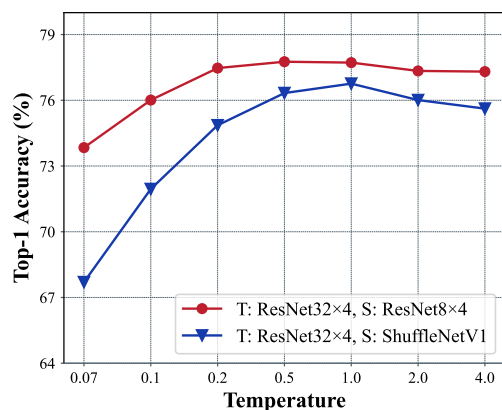


Fig. 7. Comparison of temperatures on CIFAR-100. Experiments are conducted on (1) ResNet8 $\times$ 4 and ResNet32 $\times$ 4, (2) ShuffleNetV1 and ResNet32 $\times$ 4.

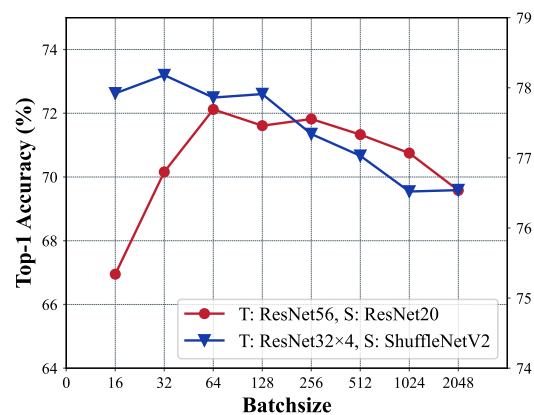


Fig. 8. Comparison of batch sizes on CIFAR-100. Experiments are conducted on (1) ResNet8 $\times$ 4 and ResNet32 $\times$ 4, (2) ShuffleNetV1 and ResNet32 $\times$ 4.

dataset. Table III and Table IV report experimental results on the ImageNet-1K dataset. We can see that our method achieves superior performance with both teacher-student architectures. Moreover, the performance of CKD surpasses state-of-the-art

results, providing further evidence of the effectiveness of our approach. Specifically, the proposed CKD achieves accuracy improvements of 1.58% and 4.39% over vanilla KD with the same and different teacher-student architectures.

TABLE VII  
 ABLATION STUDIES OF TRIPLE DESIGN ON THE CIFAR-100 DATASET. EXPERIMENTS ARE CONDUCTED ON BOTH HOMOGENEOUS AND HETEROGENEOUS TEACHER-STUDENT PAIRS. DUE TO THE FIXED TEACHER, TRIPLES  $(t_i, s_i, t_j)$  IS MEANINGLESS AND EXCLUDED FROM THIS TABLE.

Triples	Homogeneous architectures			Heterogeneous architectures		
Teacher	ResNet56 72.34	WRN-40-2 75.61	WRN-40-2 75.61	VGG13 74.64	ResNet50 79.34	ResNet32×4 79.42
Student	ResNet20 69.06	WRN-16-2 73.26	WRN-40-1 71.98	MobileNetV2 64.60	MobileNetV2 64.60	ShuffleNetV2 71.82
CKD( $s_i, t_i, s_j$ )	71.76	75.31	74.40	70.04	68.93	78.02
CKD( $s_i, t_i, t_j$ )	71.69	75.88	74.43	70.09	69.68	77.06
CKD( $t_i, s_i, s_j$ )	<b>72.12</b>	<b>76.28</b>	<b>75.14</b>	<b>70.11</b>	<b>70.62</b>	<b>78.18</b>

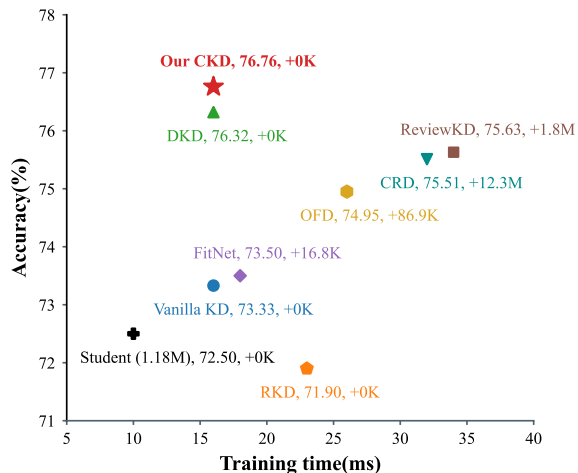


Fig. 9. Comparison of training time per batch and accuracy on CIFAR-100. The teacher model is ResNet32×4 and the student model is ResNet8×4. Additional parameters are denoted after +, which are added based on the student’s foundation.

## B. Object Detection

1) *Datasets*: We conduct experiments on the MS-COCO dataset [43]. MS-COCO is a popular dataset featuring 80 categories, divided into two subsets, including a training set of 118,000 images and a validation set of 5,000 images.

2) *Experimental Setup*: We analyze ResNet-101 & ResNet-18, ResNet-101 & ResNet-50, and ResNet-50 & MobileNetV2 teacher-student pairs. Moreover, we evaluate the MS-COCO validation set with the baseline provided by Detectron2.

3) *Implementation Details*: Experiments are performed on NVIDIA RTX 3090. We utilize Faster R-CNN with FPN as the feature extractor and implement CKD on the R-CNN head. We set  $\alpha$  to 0.1 and the temperature  $\tau$  to 1.0. Schedulers and task-specific loss settings are following Detectron2.

4) *Performance on MS-COCO*: Table V presents the object detection results on the MS-COCO dataset under three teacher-student settings. We can see that the proposed approach obtains comparable performance against logit-based approaches but inferior performance compared to feature-based approaches, particularly for ReviewKD. Object detection relies on spatial representations to locate objects. However, logits lack detailed spatial information [36], [76]. ReviewKD [7] conducts multi-

level feature distillation, resulting in better performance. We combine ReviewKD with logit-based approaches to utilize spatial information. Notably, the combined approaches, including CKD+ReviewKD and DKD+ReviewKD, significantly improve object detection results compared to previous counterparts.

## C. Ablation Study

1) *Effects of Temperature  $\tau$* : In the training phase, a high  $\tau$  yields a smooth distribution across classes, making distillation more challenging. But, a low  $\tau$  leads to a sharp distribution. To investigate the effect of  $\tau$  on CKD, we conduct ablation studies by using ResNet32×4 & ResNet8×4 and ResNet32×4 & ShuffleNetV1 pairs. Typically,  $\tau$  is set to a low value within a range of 0.07 to 4.0, while other parameters are kept constant.

Fig. 7 presents Top-1 classification accuracies for different temperatures  $\tau$ . We can observe that our method performs best when temperature  $\tau$  is around 1.0 and performs poorly when  $\tau$  is low or high. This suggests that our method is better suited for aligning  $t_i$  and  $s_i$  when the value of  $\tau$  is near 1.0.

From Theorem 1, we conclude that the gradient  $\nabla_{s_*} \mathcal{L}_i$  is proportional to  $g_i$ . When  $\tau < 1$ , the difference between  $e^{f(t_i, s_i)/\tau}$  and  $e^{f(t_i, s_j)/\tau}$  is magnified exponentially. In the limit, we obtain  $\lim_{\tau \rightarrow 0} g_i = 0$ . As a result,  $g_i$  approaches zero, causing a rapid decline in performance. When  $\tau > 1$ , the difference is lessened and  $g_i$  becomes more sensitive to negative samples as  $\lim_{\tau \rightarrow \infty} g_i = \frac{B}{B+1}$ .

2) *Effects of Batchsize*: To analyze the effect of batch size, we utilize two teacher-student pairs including ResNet56 & ResNet20 and ResNet32×4 & ShuffleNetV2. Moreover, we set the batch size to  $2^k$ , where  $k \in [4, 11] \cap k \in \mathbb{N}$ .

Fig. 8 presents Top-1 classification performance with varying batch sizes. We can see that our method attains good performance when the batch size is 64 for ResNet56 & ResNet20 and 32 for ResNet32×4 & ShuffleNetV2. Larger or smaller batch sizes are not optimal.

We also find that a large batch size potentially hampers the efficacy of our method as it affects intra-sample alignment through an increased  $\beta$ . However, a small batch size can lead to insufficient gradient magnitude. In fact, the optimal batch size for the sample-wise formulation is strongly correlated with the number of categories. It should be smaller than the number of categories to avoid neglecting intra-sample distillation and facilitate effective inter-sample distillation.

TABLE VIII

CLASSIFICATION ACCURACY (%) ON THE CIFAR-100 VALIDATION SET. WRN-16-2 IS USED AS A STUDENT. IN THE LEFT-HAND SECTION OF THE TABLE, WRN SERIES NETWORKS SERVE AS TEACHERS, WHILE IN THE RIGHT-HAND SECTION, DIFFERENT SERIES NETWORKS ARE UTILIZED AS TEACHERS.

Methods	WRN Series			Different Series		
Teacher	WRN-40-2	WRN-16-4	WRN-28-4	VGG13	WRN-16-4	ResNet50
	75.61	77.21	79.12	74.64	77.21	79.34
Studnet	73.26	73.26	73.26	73.26	73.26	73.26
vanilla KD [25]	74.92	76.00	75.14	74.30	76.00	74.62
CKD	<b>76.28</b>	<b>76.22</b>	<b>76.42</b>	<b>75.14</b>	<b>76.22</b>	<b>76.45</b>

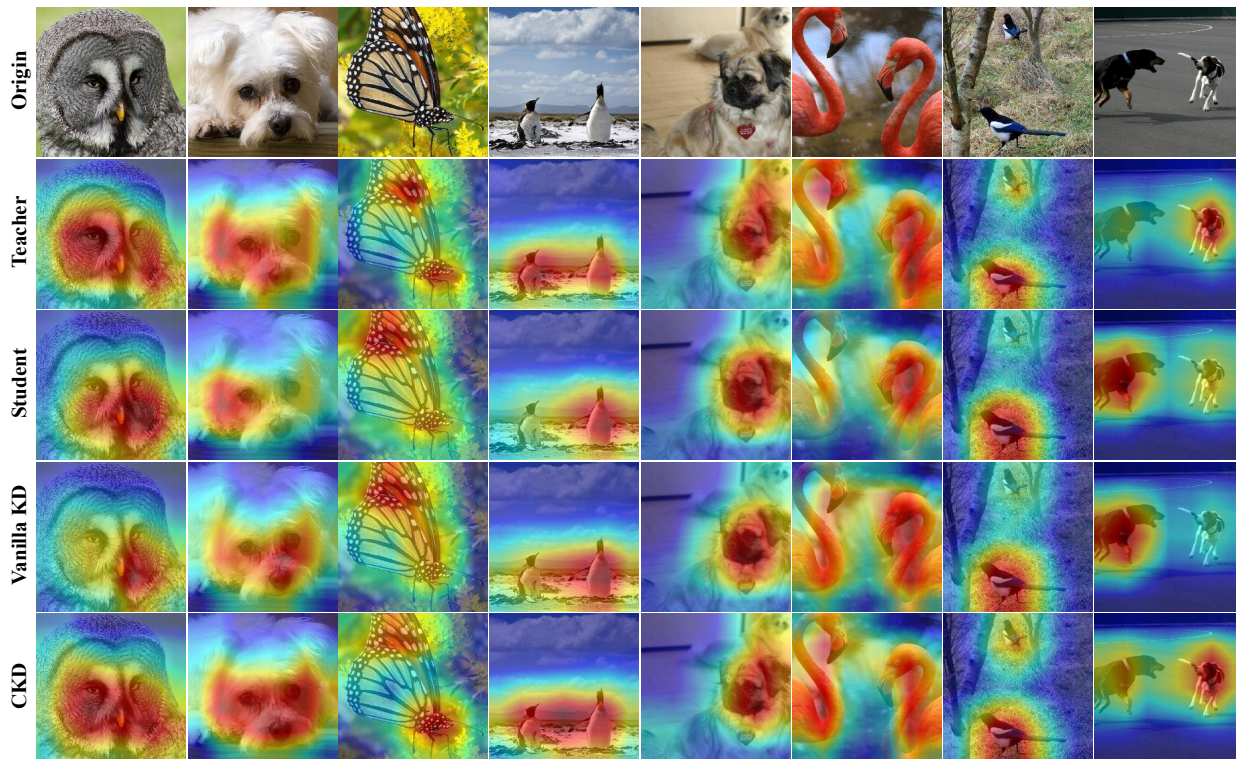


Fig. 10. Class Activation Map via GradCAM. The teacher networks (ResNet34) and the student networks (ResNet18) are trained on ImageNet-1K.

3) *Influence of Contrastive Formulation*: Fig. 6 visualizes class-wise and sample-wise contrastive formulations. SupCon [28] is a class-wise approach that selects positive pairs within the same class. Note that CRD [70] is a typical class-wise method with positive pairs from the same sample and negative pairs from different classes. In contrast, CKD chooses negative pairs from different samples but potentially from the same class.

Table VI presents classification performance under different formulations. We can observe that CKD outperforms SupCon and CRD because it uses sample-wise negative samples. Moreover, CRD exploits a memory bank to access a large number of negative samples and achieves a higher accuracy than SupCon.

4) *Influence of Triple Design*: In knowledge distillation, the element of triples can be sampled from teacher or student models. Hence, there are several kinds of triples, including  $(s_i, t_i, s_j)$ ,  $(s_i, t_i, t_j)$ ,  $(t_i, s_i, t_j)$  and  $(t_i, s_i, s_j)$ .

means that we align  $s_i$  and  $t_i$  while distancing  $s_i$  from  $s_j$ . This triple can be implemented by modifying diagonal elements of the affinity matrix with  $s_i$  and  $t_i$ . Due to fixed teacher logits,  $(t_i, s_i, t_j)$  equals intra-sample alignment.

Table VII shows the classification performance with different triples. We can see that the utilization of triples  $(t_i, s_i, s_j)$  yields better performance than the other triples. Our method anchors on  $t_i$ , pulling  $s_i$  closer while pushing  $s_j$  apart. This objective is clear and simple. However, as discussed in Section III-B, triples  $(s_i, t_i, t_j)$  may cause gradient conflict. For triples  $(s_i, t_i, s_j)$ , this strategy mainly performs contrastive learning in the student logits space.

#### D. More Analyses

1) *Training Efficiency*: To evaluate the training efficiency of our approach, we compare its accuracy and parameter count against state-of-the-art methods on the CIFAR-100 dataset. Fig. 9 depicts training time per batch and classification perfor-



mance. We can observe that our method exhibits high training efficiency, striking a balance between model parameters and classification performance. Typically, feature-based methods require more parameters and longer training times than logit-based methods. ReviewKD and CRD, in particular, take twice the training time compared to our method, due to multi-level feature review and memory bank usage.

2) *Effects of Teacher Capacity*: Previous works [10], [74] have found that large teacher models may not be optimal for smaller student models due to disparities in parameters and capacity. Therefore, we further conduct experiments to analyze the influence of teacher networks with different capacities.

Table VIII presents classification performance on the CIFAR-100 dataset. We can see that our method achieves comparable performance across different WRN models, whereas vanilla KD exhibits variation in performance. Wide Residual Networks [73], is a ResNet variant. Therefore, our method also obtains an accuracy on par with ResNet50 as the teacher model, while vanilla KD has the second-worst performance. For vanilla KD, larger models lead to performance degeneration, for example, the accuracies of WRN-16-4 and WRN-28-4 are 76.00 and 75.14, respectively. Both the proposed method and vanilla KD perform poorly with the VGG13 architecture. Ablation studies prove that our method can partially mitigate the parameter and capacity gaps of larger models.

### E. Visualizations

GradCAM identifies image regions critical for concept prediction. To evaluate the consistency of CKD with teacher networks, we employ GradCAM to visualize class activation maps in Fig. 10. The teacher-student pair, including ResNet34 and ResNet18, are trained on the ImageNet-1K dataset. We can observe that our method effectively handles complex scenes and multiple objects. For example, in the seventh column, two birds are present. Our method accurately replicates teacher knowledge by focusing on both birds, whereas student networks and vanilla KD focus only on the bird closer to the camera.

## V. CONCLUSION

In this paper, we have presented a contrastive knowledge distillation approach for image classification and object detection. To be specific, we formulate knowledge distillation as a logit alignment problem, mimicking the intra-sample numerical value and inter-sample semantic structure of teacher models. By converting the structure-preserving alignment into a sample-wise contrastive learning framework, our approach can be effectively and efficiently trained with well-designed positive and negative pairs. Experimental results demonstrate that our method achieves highly competitive performance against state-of-the-art methods on benchmark datasets. In the future, we will attempt to apply the proposed method to distill large models.

## REFERENCES

- [1] G. Aguilar, Y. Ling, Y. Zhang, B. Yao, X. Fan, and C. Guo, "Knowledge distillation from internal representations," in *AAAI*, 2020, pp. 7350–7357.
- [2] Z. Allen-Zhu and Y. Li, "Towards understanding ensemble, knowledge distillation and self-distillation in deep learning," in *ICLR*, 2023, pp. 1–12.
- [3] P. Bachman, R. D. Hjelm, and W. Buchwalter, "Learning representations by maximizing mutual information across views," in *NeurIPS*, 2019, pp. 15 509–15 519.
- [4] T. Bai, J. Chen, J. Zhao, B. Wen, X. Jiang, and A. Kot, "Feature distillation with guided adversarial contrastive learning," *arXiv preprint arXiv:2009.09922*, 2020.
- [5] L. Beyer, X. Zhai, A. Royer, L. Markeeva, R. Anil, and A. Kolesnikov, "Knowledge distillation: A good teacher is patient and consistent," in *CVPR*, 2022, pp. 10925–10934.
- [6] D. Chen, J.-P. Mei, H. Zhang, C. Wang, Y. Feng, and C. Chen, "Knowledge distillation with the reused teacher classifier," in *CVPR*, 2022, pp. 11933–11942.
- [7] P. Chen, S. Liu, H. Zhao, and J. Jia, "Distilling knowledge via knowledge review," in *CVPR*, 2021, pp. 5008–5017.
- [8] T. Chen, S. Kornblith, M. Norouzi, and G. Hinton, "A simple framework for contrastive learning of visual representations," in *ICML*, 2020, pp. 1597–1607.
- [9] X. Cheng, Z. Rao, Y. Chen, and Q. Zhang, "Explaining knowledge distillation by quantifying the knowledge," in *CVPR*, 2020, pp. 12925–12935.
- [10] J. H. Cho and B. Hariharan, "On the efficacy of knowledge distillation," in *ICCV*, 2019, pp. 4794–4802.
- [11] Y. Cho, G. Ham, J.-H. Lee, and D. Kim, "Ambiguity-aware robust teacher (art): Enhanced self-knowledge distillation framework with pruned teacher network," *PR*, vol. 140, pp. 1–12, 2023.
- [12] K. Cui, Y. Yu, F. Zhan, S. Liao, S. Lu, and E. P. Xing, "KD-DLGAN: Data limited image generation via knowledge distillation," in *CVPR*, 2023, pp. 3872–3882.
- [13] J. Deng, W. Dong, R. Socher, L.-J. Li, K. Li, and L. Fei-Fei, "ImageNet: A large-scale hierarchical image database," in *CVPR*, 2009, pp. 248–255.
- [14] P. Dong, L. Li, and Z. Wei, "DisWOT: Student architecture search for distillation without training," in *CVPR*, 2023, pp. 11 898–11 908.
- [15] J. Gou, B. Yu, S. J. Maybank, and D. Tao, "Knowledge distillation: A survey," *IJCV*, vol. 129, pp. 1789–1819, 2021.
- [16] Z. Guo, W. Shiao, S. Zhang, Y. Liu, N. V. Chawla, N. Shah, and T. Zhao, "Linkless link prediction via relational distillation," in *ICML*, 2023, pp. 12012–12033.
- [17] Z. Guo, H. Yan, H. Li, and X. Lin, "Class attention transfer based knowledge distillation," in *CVPR*, 2023, pp. 11 868–11 877.
- [18] M. U. Gutmann and A. Hyvärinen, "Noise-contrastive estimation of unnormalized statistical models, with applications to natural image statistics," *JMLR*, vol. 13, no. 2, pp. 307–361, 2012.
- [19] Z. Hao, J. Guo, K. Han, H. Hu, C. Xu, and Y. Wang, "VanillaKD: Revisit the power of vanilla knowledge distillation from small scale to large scale," *arXiv preprint arXiv:2305.15781*, 2023.
- [20] Z. Hao, J. Guo, K. Han, Y. Tang, H. Hu, Y. Wang, and C. Xu, "One-for-All: Bridge the gap between heterogeneous architectures in knowledge distillation," in *NeurIPS*, 2023, pp. 1–13.
- [21] K. He, H. Fan, Y. Wu, S. Xie, and R. Girshick, "Momentum contrast for unsupervised visual representation learning," in *CVPR*, 2020, pp. 9729–9738.
- [22] K. He, X. Zhang, S. Ren, and J. Sun, "Deep residual learning for image recognition," in *CVPR*, 2016, pp. 770–778.
- [23] O. Henaff, "Data-efficient image recognition with contrastive predictive coding," in *ICML*, 2020, pp. 4182–4192.
- [24] B. Heo, J. Kim, S. Yun, H. Park, N. Kwak, and J. Y. Choi, "A comprehensive overhaul of feature distillation," in *ICCV*, 2019, pp. 1921–1930.
- [25] G. Hinton, O. Vinyals, and J. Dean, "Distilling the knowledge in a neural network," *arXiv preprint arXiv:1503.02531*, 2015.
- [26] T. Huang, S. You, F. Wang, C. Qian, and C. Xu, "Knowledge distillation from a stronger teacher," *NeurIPS*, vol. 35, pp. 33 716–33 727, 2022.
- [27] Y. Jin, J. Wang, and D. Lin, "Multi-level logit distillation," in *CVPR*, 2023, pp. 24 276–24 285.
- [28] P. Khosla, P. Teterwak, C. Wang, A. Sarna, Y. Tian, P. Isola, A. Maschinot, C. Liu, and D. Krishnan, "Supervised contrastive learning," *NeurIPS*, vol. 33, pp. 18 661–18 673, 2020.
- [29] Y. Kim, J. Park, Y. Jang, M. Ali, T.-H. Oh, and S.-H. Bae, "Distilling global and local logits with densely connected relations," in *ICCV*, 2021, pp. 6290–6300.
- [30] M. Klingner, S. Borse, V. R. Kumar, B. Rezaei, V. Narayanan, S. Yogamani, and F. Porikli, "X3KD: Knowledge distillation across modalities, tasks and stages for multi-camera 3d object detection," in *CVPR*, 2023, pp. 13 343–13 353.
- [31] N. Komodakis and S. Zagoruyko, "Paying more attention to attention: improving the performance of convolutional neural networks via attention transfer," in *ICLR*, 2017, pp. 1–13.



- [32] A. Krizhevsky, "Learning multiple layers of features from tiny images," Master's thesis, University of Toronto, 2009.
- [33] J. Li, Z. Guo, H. Li, S. Han, J.-w. Baek, M. Yang, R. Yang, and S. Suh, "Rethinking feature-based knowledge distillation for face recognition," in *CVPR*, 2023, pp. 20 156–20 165.
- [34] K. Li, J. Wan, and S. Yu, "Ckdf: Cascaded knowledge distillation framework for robust incremental learning," *TIP*, vol. 31, pp. 3825–3837, 2022.
- [35] L. Li, P. Dong, Z. Wei, and Y. Yang, "Automated knowledge distillation via monte carlo tree search," in *ICCV*, 2023, pp. 17 413–17 424.
- [36] Q. Li, S. Jin, and J. Yan, "Mimicking very efficient network for object detection," in *CVPR*, 2017, pp. 6356–6364.
- [37] X. Li, S. Li, B. Omar, F. Wu, and X. Li, "Reskd: Residual-guided knowledge distillation," *TIP*, vol. 30, pp. 4735–4746, 2021.
- [38] Z. Li, X. Li, X. Fu, X. Zhang, W. Wang, S. Chen, and J. Yang, "Promptkd: Unsupervised prompt distillation for vision-language models," in *CVPR*, 2024.
- [39] Z. Li, X. Li, L. Yang, B. Zhao, R. Song, L. Luo, J. Li, and J. Yang, "Curriculum temperature for knowledge distillation," in *AAAI*, 2023, pp. 1504–1512.
- [40] Z. Li, P. Xu, X. Chang, L. Yang, Y. Zhang, L. Yao, and X. Chen, "When object detection meets knowledge distillation: A survey," *TPAMI*, vol. 45, no. 8, pp. 10 555–10 579, 2023.
- [41] H. Lin, G. Han, J. Ma, S. Huang, X. Lin, and S.-F. Chang, "Supervised masked knowledge distillation for few-shot transformers," in *CVPR*, 2023, pp. 19 649–19 659.
- [42] S. Lin, H. Xie, B. Wang, K. Yu, X. Chang, X. Liang, and G. Wang, "Knowledge distillation via the target-aware transformer," in *CVPR*, 2022, pp. 10 915–10 924.
- [43] T.-Y. Lin, M. Maire, S. Belongie, J. Hays, P. Perona, D. Ramanan, P. Dollár, and C. L. Zitnick, "Microsoft coco: Common objects in context," in *ECCV*, 2014, pp. 740–755.
- [44] L. Liu, Q. Huang, S. Lin, H. Xie, B. Wang, X. Chang, and X. Liang, "Exploring inter-channel correlation for diversity-preserved knowledge distillation," in *ICCV*, 2021, pp. 8271–8280.
- [45] Y. Liu, K. Chen, C. Liu, Z. Qin, Z. Luo, and J. Wang, "Structured knowledge distillation for semantic segmentation," in *CVPR*, 2019, pp. 2604–2613.
- [46] Y. Liu, J. Cao, B. Li, C. Yuan, W. Hu, Y. Li, and Y. Duan, "Knowledge distillation via instance relationship graph," in *CVPR*, 2019, pp. 7096–7104.
- [47] N. Ma, X. Zhang, H.-T. Zheng, and J. Sun, "Shufflenet v2: Practical guidelines for efficient cnn architecture design," in *ECCV*, 2018, pp. 116–131.
- [48] C. Meng, R. Rombach, R. Gao, D. Kingma, S. Ermon, J. Ho, and T. Salimans, "On distillation of guided diffusion models," in *CVPR*, 2023, pp. 14 297–14 306.
- [49] A. K. Menon, A. S. Rawat, S. Reddi, S. Kim, and S. Kumar, "A statistical perspective on distillation," in *ICML*, 2021, pp. 7632–7642.
- [50] R. Miles, M. K. Yucel, B. Manganeli, and A. Saà-Garriga, "MobileVOS: Real-time video object segmentation contrastive learning meets knowledge distillation," in *CVPR*, 2023, pp. 10 480–10 490.
- [51] S. I. Mirzadeh, M. Farajtabar, A. Li, N. Levine, A. Matsukawa, and H. Ghasemzadeh, "Improved knowledge distillation via teacher assistant," in *AAAI*, 2020, pp. 5191–5198.
- [52] Y. Niu, L. Chen, C. Zhou, and H. Zhang, "Respecting transfer gap in knowledge distillation," *NeurIPS*, vol. 35, pp. 21 933–21 947, 2022.
- [53] U. Ojha, Y. Li, A. Sundara Rajan, Y. Liang, and Y. J. Lee, "What knowledge gets distilled in knowledge distillation?" *NeurIPS*, pp. 1–12, 2024.
- [54] A. v. d. Oord, Y. Li, and O. Vinyals, "Representation learning with contrastive predictive coding," *arXiv preprint arXiv:1807.03748*, 2018.
- [55] W. Park, D. Kim, Y. Lu, and M. Cho, "Relational knowledge distillation," in *CVPR*, 2019, pp. 3967–3976.
- [56] B. Peng, X. Jin, J. Liu, D. Li, Y. Wu, Y. Liu, S. Zhou, and Z. Zhang, "Correlation congruence for knowledge distillation," in *ICCV*, 2019, pp. 5007–5016.
- [57] M. Phuong and C. Lampert, "Towards understanding knowledge distillation," in *ICML*, 2019, pp. 5142–5151.
- [58] A. Radford, J. W. Kim, C. Hallacy, A. Ramesh, G. Goh, S. Agarwal, G. Sastry, A. Askell, P. Mishkin, J. Clark *et al.*, "Learning transferable visual models from natural language supervision," in *ICML*, 2021, pp. 8748–8763.
- [59] A. Romero, N. Ballas, S. E. Kahou, A. Chassang, C. Gatta, and Y. Bengio, "Fitnets: Hints for thin deep nets," in *ICLR*, 2015.
- [60] M. Sandler, A. Howard, M. Zhu, A. Zhmoginov, and L.-C. Chen, "Mobilenetv2: Inverted residuals and linear bottlenecks," in *CVPR*, 2018, pp. 4510–4520.
- [61] Z. Shen and E. Xing, "A fast knowledge distillation framework for visual recognition," in *ECCV*, 2022, pp. 673–690.
- [62] C. Shu, Y. Liu, J. Gao, Z. Yan, and C. Shen, "Channel-wise knowledge distillation for dense prediction," in *ICCV*, 2021, pp. 5311–5320.
- [63] K. Simonyan and A. Zisserman, "Very deep convolutional networks for large-scale image recognition," in *ICLR*, 2015.
- [64] K. Sohn, "Improved deep metric learning with multi-class n-pair loss objective," *NeurIPS*, vol. 29, pp. 1–9, 2016.
- [65] J. Song, Y. Chen, J. Ye, and M. Song, "Spot-adaptive knowledge distillation," *TIP*, vol. 31, pp. 3359–3370, 2022.
- [66] S. Stanton, P. Izmailov, P. Kirichenko, A. A. Alemi, and A. G. Wilson, "Does knowledge distillation really work?" *NeurIPS*, vol. 34, pp. 6906–6919, 2021.
- [67] S. Sun, W. Ren, J. Li, R. Wang, and X. Cao, "Logit standardization in knowledge distillation," *CVPR*, 2024.
- [68] J. Tang, R. Shivanna, Z. Zhao, D. Lin, A. Singh, E. H. Chi, and S. Jain, "Understanding and improving knowledge distillation," *arXiv preprint arXiv:2002.03532*, 2020.
- [69] Y. Tian, D. Krishnan, and P. Isola, "Contrastive multiview coding," in *ECCV*, 2020, pp. 776–794.
- [70] Y. Tian, D. Krishnan, and P. Isola, "Contrastive representation distillation," in *ICLR*, 2020, pp. 1–12.
- [71] Z. Tu, X. Liu, and X. Xiao, "A general dynamic knowledge distillation method for visual analytics," *TIP*, vol. 31, pp. 6517–6531, 2022.
- [72] F. Tung and G. Mori, "Similarity-preserving knowledge distillation," in *ICCV*, 2019, pp. 1365–1374.
- [73] S. Zagoruyko and N. Komodakis, "Wide residual networks," *arXiv preprint arXiv:1605.07146*, 2016.
- [74] L. Wang and K.-J. Yoon, "Knowledge distillation and student-teacher learning for visual intelligence: A review and new outlooks," *TPAMI*, vol. 44, no. 6, pp. 3048–3068, 2021.
- [75] R. Wang, Y. Hao, L. Hu, X. Li, M. Chen, Y. Miao, and I. Humar, "Efficient crowd counting via dual knowledge distillation," *TIP*, vol. 33, pp. 569–583, 2023.
- [76] T. Wang, L. Yuan, X. Zhang, and J. Feng, "Distilling object detectors with fine-grained feature imitation," in *CVPR*, 2019, pp. 4933–4942.
- [77] T. Wang and P. Isola, "Understanding contrastive representation learning through alignment and uniformity on the hypersphere," in *ICML*, 2020, pp. 9929–9939.
- [78] Z. Wu, Y. Xiong, S. X. Yu, and D. Lin, "Unsupervised feature learning via non-parametric instance discrimination," in *CVPR*, 2018, pp. 3733–3742.
- [79] G. Xu, Z. Liu, X. Li, and C. C. Loy, "Knowledge distillation meets self-supervision," in *ECCV*, 2020, pp. 588–604.
- [80] C. Yang, Z. An, H. Zhou, F. Zhuang, Y. Xu, and Q. Zhang, "Online knowledge distillation via mutual contrastive learning for visual recognition," *TPAMI*, vol. 45, no. 8, pp. 10 212–10 227, 2023.
- [81] C. Yang, H. Zhou, Z. An, X. Jiang, Y. Xu, and Q. Zhang, "Cross-image relational knowledge distillation for semantic segmentation," in *CVPR*, 2022, pp. 12 319–12 328.
- [82] Z. Yang, Z. Li, X. Jiang, Y. Gong, Z. Yuan, D. Zhao, and C. Yuan, "Focal and global knowledge distillation for detectors," in *CVPR*, 2022, pp. 4643–4652.
- [83] Z. Yang, A. Zeng, C. Yuan, and Y. Li, "From knowledge distillation to self-knowledge distillation: A unified approach with normalized loss and customized soft labels," in *ICCV*, 2023, pp. 17 185–17 194.
- [84] C.-H. Yeh, C.-Y. Hong, Y.-C. Hsu, T.-L. Liu, Y. Chen, and Y. LeCun, "Decoupled contrastive learning," in *ECCV*, 2022, pp. 668–684.
- [85] S. Zagoruyko and N. Komodakis, "Paying more attention to attention: Improving the performance of convolutional neural networks via attention transfer," *arXiv preprint arXiv:1612.03928*, 2016.
- [86] L. Zhang and X. Wu, "Latent space semantic supervision based on knowledge distillation for cross-modal retrieval," *TIP*, vol. 31, pp. 7154–7164, 2022.
- [87] L. Zhang, R. Dong, H.-S. Tai, and K. Ma, "Pointdistiller: Structured knowledge distillation towards efficient and compact 3d detection," in *CVPR*, 2023, pp. 21 791–21 801.
- [88] X. Zhang, X. Zhou, M. Lin, and J. Sun, "Shufflenet: An extremely efficient convolutional neural network for mobile devices," in *CVPR*, 2018, pp. 6848–6856.
- [89] Y. Zhang, T. Xiang, T. M. Hospedales, and H. Lu, "Deep mutual learning," in *CVPR*, 2018, pp. 4320–4328.
- [90] B. Zhao, Q. Cui, R. Song, Y. Qiu, and J. Liang, "Decoupled knowledge distillation," in *CVPR*, 2022, pp. 11 953–11 962.